Relevance analysis of AEB control strategy and occupant kinematics based on typical cut-in scenario

Chengyue Jiang , Xiangzhi Meng , Lihai Ren , Xi Liu & Chen Li

Taylor & Francis
Taylor & Francis Group

Relevance analysis of AEB control strategy and occupant kinematics based on typical cut-in scenario

Chengyue Jiang[a,b], Xiangzhi Meng[b], Lihai Ren[b], Xi Liu[b] and Chen Li[b]

[a]State Key Laboratory of Vehicle NVH and Safety Technology, Chongqing, China; [b]Key Laboratory of Advanced Manufacture Technology for Automobile Parts, Ministry of Education, Chongqing University of Technology, Chongqing, China

ABSTRACT

The objective of this study was to explore the relevance between Autonomous Emergency Braking (AEB) control strategy and occupant pre-impact kinematics among a typical real-world cut-in impact scenario. First, the accident scenario was built with PreScan software after accident analysis. Second, a MADYMO simulation model with Active Human Model (AHM) was built and validated with the volunteer test carried out by our team. Finally, the AEB module and related control strategies were introduced into the main vehicle, and the effects of different strategies on the occupant kinematic were evaluated. The simulation results indicated that it was efficient to evaluate the occupant kinematics during pre-impact phase through vehicle and occupant integrated simulation method. The main vehicle's velocity could be reduced between 5 km/h and 14 km/h respectively after introducing different AEB control strategies, which was less than the one manoeuvred by driver (22 km/h). Earlier activation of the AEB and heavier braking could result in larger up-body displacement, but less final impact velocity, and the maximum head displacement reached 172.56 mm due to the AEB control. Comparing partial braking with detection angle 9° case with 100% braking with detection angle 18° case, the head, thorax and shoulder displacements were increased by 94.8%, 104.1%, and 48.7%. This research is beneficial for the subsequent integrated safety analysis.

1. Introduction

Road traffic injuries are currently the leading cause of death for children and young adults aged 5–29 years, and the number of deaths on the world's roads remains unacceptably high, with an estimated 1.35 million people dying each year [1]. Continuous efforts have been made to improve vehicle safety and mitigate the road traffic injuries [2–6]. With the advent of vehicle active safety technologies, researchers and engineers have become increasingly interested in preventing accidents by Advance Driver Assistance Systems (ADAS) [7, 8]. The ADAS can brake automatically and influence the vehicle's kinematics before impact and so they can avoid or mitigate accidents [9]. Based on surveys analysing the cause of traffic accidents, ADAS features have the potential to reduce vehicle traffic accidents by up to 40% [10].

Among ADAS, the Autonomous Emergency Braking (AEB) seems to be a future key to improve vehicle passenger safety, which can reduce collision speeds, and therefore severity levels significantly [11,12]. Recently, more vehicle models are equipped with the AEB system. The effectiveness of AEB in collision damage mitigation is usually assessed in a proving ground following a prescribed test protocol.

While in the reality, there may be various situations in which AEB can be activated, and the occupant posture can be changed by braking manoeuvres as well [13]. Bastien et al. [14] proposed a new set of generic biomechanical kinematic responses based on sled test data, and provided new kinematics corridors for head and torso angular change in a typical '1 g' frontal scenario. Riske Meijer et al. [15] indicated that the active human model responses differed significantly with that of a dummy model in a far-side impact. van Rooij et al. [16] performed a study with a professional driver under braced as well as unbraced conditions, attentive braking by the driver led to forward displacements between 37 and 128 mm, whereas automatic braking at distracted conditions led to an average forward displacement of 123 mm. Such changes of driver's posture and velocity during emergency manoeuvres exert influence on the injury risks in frontal impact collisions [17].

The objective of this study was to evaluate occupant posture changes during pre-impact braking and explain effects of AEB control strategy on occupant kinematics. In order to build the pre-crash circumstance, a typical cut-in scenario was reconstructed with the PreScan software according to a real-world accident. The MADYMO simulation model including the Active Human Model (AHM) was built and

CONTACT Xi Liu ✉ liuxi@cqut.edu.cn 🏛 Key Laboratory of Advanced Manufacture Technology for Automobile Parts, Ministry of Education, Chongqing University of Technology, No. 69 Hong Guang Da Dao, Ba Nan Qu, Chongqing 400054, China
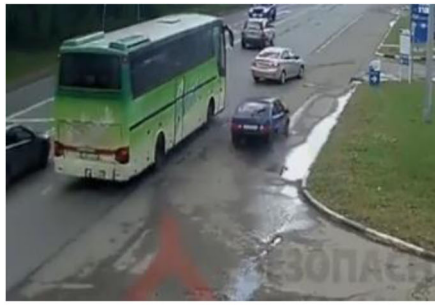
(a) Pre-impact scenario

(b) Impact moment

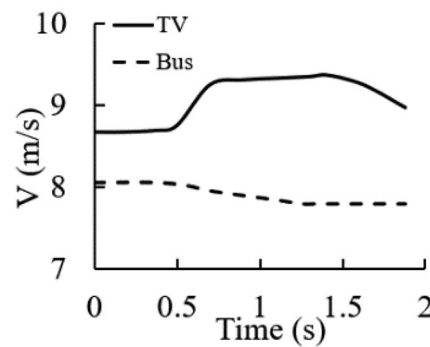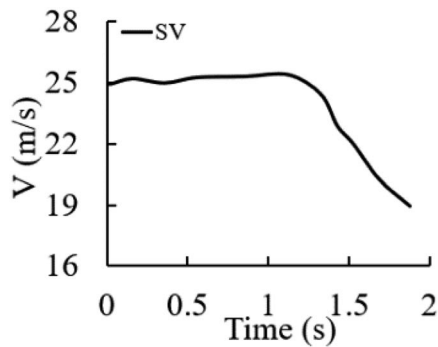**Figure 1.** Cut-in accident scenario.

Figure 2. Vehicle velocities among the cut-in accident.

correlated with the volunteer test results. Then the AEB module was introduced into the accident scenario and different control strategies' effects on both vehicle longitudinal velocities and occupant longitudinal displacements were evaluated.

2 Method

2.1. Accident analysis and scenario reconstruction

The vehicle cut-in scenario for this study is based on a real traffic accident case. According to the road camera, the frontal target vehicle (TV) changed the lane suddenly towards the gas station, while the rear main vehicle (SV) was driving in the right lane with a higher speed at initial moment (Figure 1a). The driver's vision of SV was blocked by the bus, and he took braking manoeuvre immediately after detecting the TV's cut-in manoeuvre. The impact occurred due to the high relative speed (Figure 1b).

The frame rate for this road camera was 15 fps, which indicated the time interval of each frame was 0.067 s. The main features of vehicles including wheel-base were visible in the video, and the vehicle motion could be tracked frame by frame. The vehicle velocity in this case was calculated by the moving ruler time interpolation method [18], as shown in Equation 1.

$$V = \frac{Lf}{n + \Delta t_1} \qquad (1)$$

Where L is wheel-base, n is frame number, f is frame rate, Δt_1 is interpolation time.

After analysing the vehicle motion through video analysis and calculating the Δt_1 of the video, the velocity of each vehicle could be obtained (Figure 2). The initial velocity of SV was about 90 km/h (25.0 m/s), and the velocity change of SV due to driver manoeuvre was around 22 km/h (6.1 m/s).

The PreScan software was used to reconstruct the accident scene, including a five-lane road with a length of 100 metres, two vehicles and a bus (limited by the PreScan database, replaced by a similar truck). The vehicle path, as well as the vehicle motion was set according to the accident video, as shown in Figure 3 below.

In order to reconstruct the accident scene more realistically in the PreScan, the path follower module was applied for the vehicle motion reconstruction. To validate its accuracy, the PreScan simulation results at 0 s, 0.6 s, 1.2 s and 1.9 s were captured and compared with the corresponding frames of the accident video. The simulated animation correlated well with accident scene (Figure 4). Figure 5 illustrates the comparisons of velocities from the video analysis and the PreScan simulation, which indicated that the PreScan accident scene was reliable and could be used for subsequent research.

2.2. Volunteer test and occupant model validation

To analyse the out-of-position displacements of passengers under the emergency braking condition, a volunteer test based on a vehicle from local manufacture was carried out by our team [19]. The acceleration sensor was placed under the B-pillar to measure the deceleration of the vehicle, and the force sensors (f305-z4944) were placed at
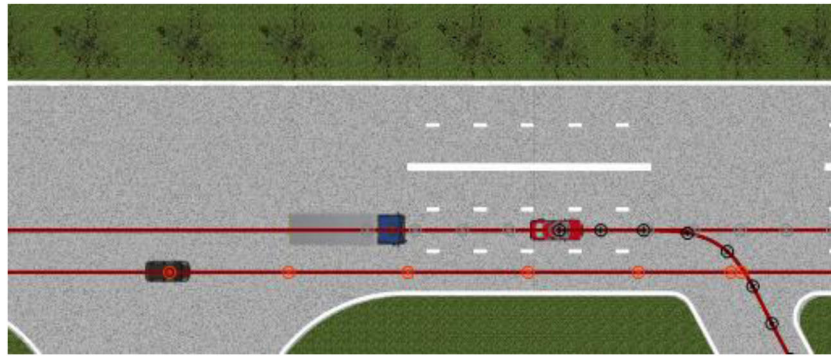
Figure 3. Accident scenario reconstruction in PreScan.
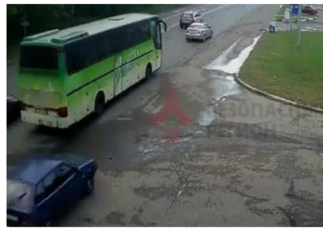
(a) 0s
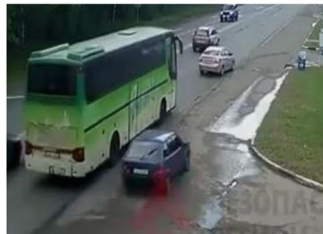
(b) 0.6s

(c) 1.2s

(d) 1.9s

Figure 4. Correlation of vehicle motion.

both shoulder belt and lap belt to record the seat belt forces. Besides, a displacement sensor was placed under the seat headrest to measure the out-of-position displacement of the occupant's thorax (T1, Figure 6a). The test data was stored in the on-board data acquisition device (Figure 6b).
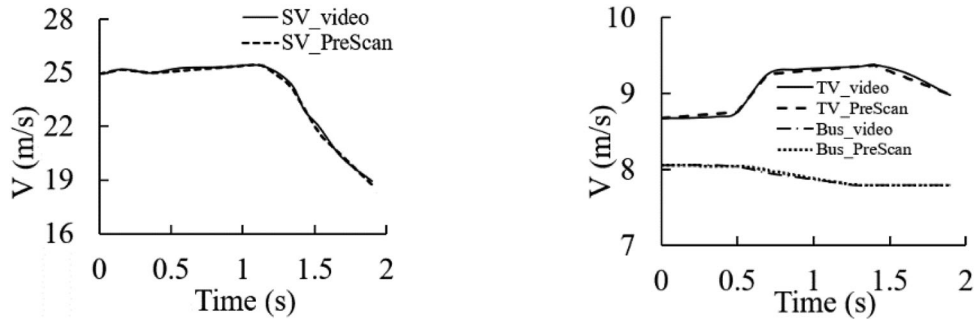
Figure 5. Validation of vehicle velocities.

(a) T1 displacement sensor (b) On-board data acquisition device

Figure 6. Volunteer test set-up.

The occupant kinematics simulation model (Figure 7) was built by using MADYMO software, which could be used to analyse the relevance between braking parameters and occupant responses. In addition to the restraint system modules, an Active Human Model (AHM) from MADYMO database was introduced for better biofidelic response, since AHM has controllers for major joints of the neck, arm, spine regions [20]. Besides, the AHM was used instead of Hybrid-III dummy because the kinematic of the Hybrid-III dummy in such scenarios turned out to be unrealistic in previous study [21]. For this reason, more and more researchers were using active human model or human FE model to study occupant kinematics and injury mechanism [22,23].

The AHM muscle model is based on the classic Hill muscle model, which simulates the human muscle movement through the contraction unit (ce) and the parallel elastic unit (pe) [24]. Two endpoints of a muscle model can be linked to bodies or any two points in the reference space. Among the muscle model, the muscle force is expressed as a function of the distance between two points (l), the elongation speed (v) and the degree of activation (A). The equations of muscle forces are as follows:

$$F = F_{ce} + F_{pe} \qquad (2)$$

$$F_{ce} = A(t)F_{max}F_H(v)F_L(l) \qquad (3)$$

$$F_{pe} = F_{max}F_p(l) \qquad (4)$$

Where, F_{ce} is the contraction unit force, F_{pe} is the parallel elastic unit force, $A(t)$ is the muscle activation level over time, F_{max} is the maximum isometric contraction force, $F_H(v)$ is the normalised active force over velocity for the contractive unit, $F_L(l)$ is the normalised active force over length for the contractive unit and $F_p(l)$ is the normalised passive force over length for the parallel elastic unit.

For this study, the parameters of F_{max}, $F_H(v)$, $F_L(l)$ and $F_P(l)$ were set according to relevant literature [25,26]. The model validation work was mainly focussing on AHM positioning and the definition of activation level. The muscle activation level $A(t)$ is between 0 and 1, which can be set over time. 0 represents no active behaviour, 1 represents the maximum tension degree [27]. For this model validation, the activation level is time dependent, as shown in Figure 8.

As shown in Figure 9, both the shoulder belt force and T1 displacement from the simulation were correlated with those from the test. The T1 displacement curve of the AHM simulation was coincident with that of the volunteer test, which indicated that AHM and the volunteer were highly consistent among the process of braking. The validated simulation model would be used for the following study.

2.3. AEB control strategy set-up

In this study, the motion of the main vehicle among the pre-impact phase could be affected by the AEB control strategy of the vehicle after introducing the AEB module. When the target vehicle could be detected, the AEB would assess their relative position and trigger corresponding braking manoeuvre in certain emergency cases. In this case, the main vehicle adopted Long Range Radar (LRR) and Short Range Radar (SRR) to monitor its relative speed and
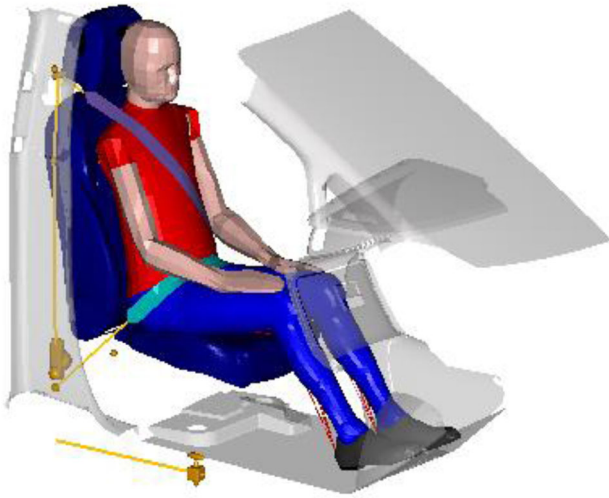

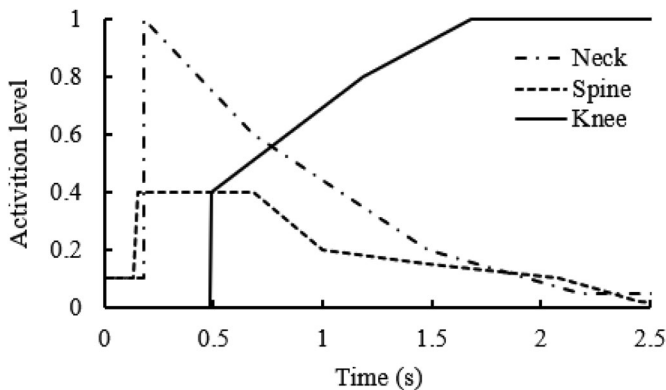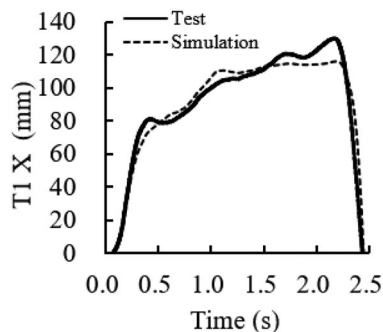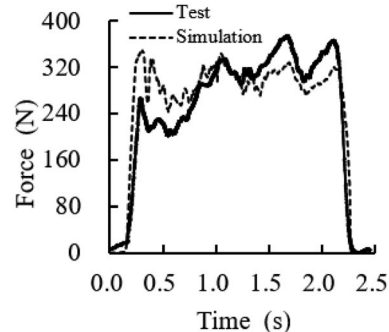Figure 7. Occupant simulation model with AHM.

Figure 8. Activation level of AHM main regions for this case.

distance with the frontal target vehicle in the PreScan simulation, and the detection angle of the LRR was set to 9° originally. The AEB system adopted the commonly used Time to Collision (TTC) algorithm to evaluate the front collision risk, as in the research of Ref. [28]. TTC algorithm focuses on the relative distance and the relative speed of two vehicles (Equation 5).

$$TTC = \frac{D_r}{V_r} \qquad (5)$$

Where D_r is relative distance, V_r is relative speed.

According to the typical cut-in scenario in this paper, four kinds of control strategies were proposed for the following study: (a) two-stage partial braking strategy (LRR angel at 9°), (b) one-stage 100% braking strategy (LRR angel at 9°), (c) two-stage partial braking strategy (LRR angel at 18°) and (d) one-stage 100% braking strategy (LRR angel at 18°). These control strategies were set according to the previous research [29], and their effects on final impact velocities and occupant kinematics would be analysed in this study, respectively. Besides, the influence of different detection angles on the AEB intervention time and braking acceleration would be analysed as well.

The vehicle dynamic module in PreScan is simple and has no hydraulic control module. For this reason, a dynamic module was introduced to simulate the change of throttle opening and braking pressure more accurately in the process of vehicle simulation. A transfer function (Equation 6) is used to make the output of braking pressure more realistic [30].

$$H(s) = \frac{1}{as + 1} \qquad (6)$$

Where a is the coefficient of time that delays the braking (in this case, $a = 0.1$), s is the input braking pressure.

The control strategy in the MATLAB/Simulink environment is shown in Figure 10.

3. Results

The SV's acceleration and final impact velocity under each control strategy during the pre-impact phase are shown in Figure 11. From the braking acceleration curves in Figure 11a, it could be seen that the activation time of AEB was
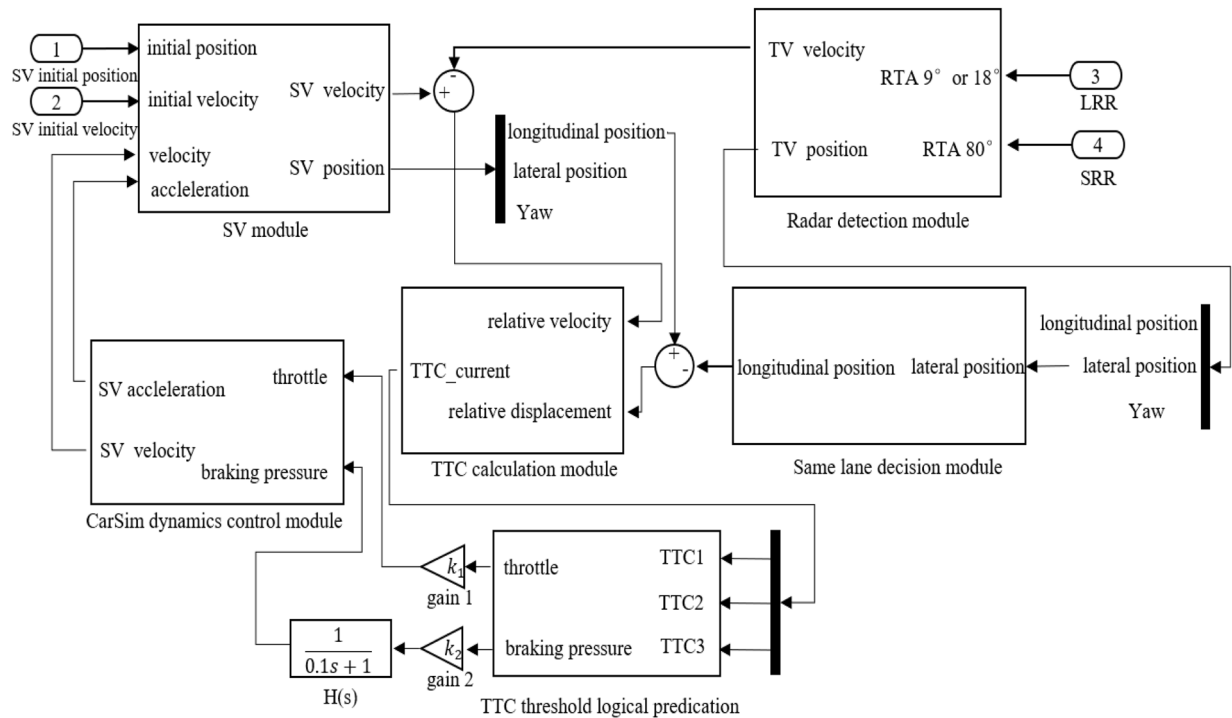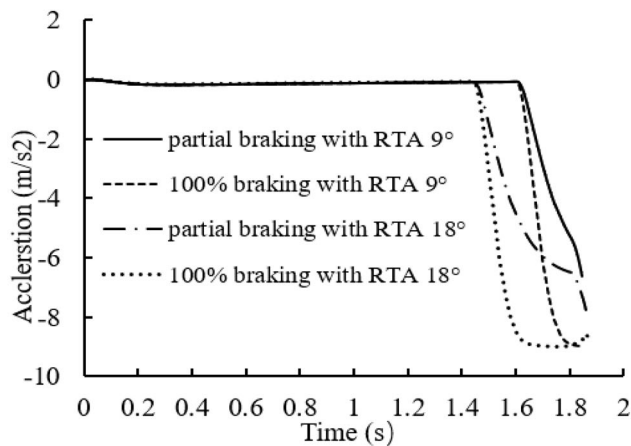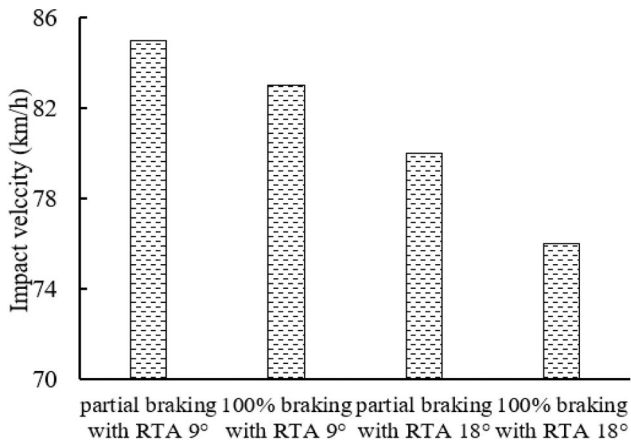

(a) Shoulder belt force correlation

(b) T1 displacement correlation

Figure 9. Belt force and T1 displacement correlation.

Figure 10. The AEB control strategy in Simulink.

(a) Vehicle acceleration curves

partial braking 100% braking partial braking 100% braking
with RTA 9° with RTA 9° with RTA 18° with RTA 18°

(b) Final impact velocities

Figure 11. Vehicle accelerations and impact velocities under different AEB control strategies.

almost the same for those with the same detection angle. The AEB activation timing under the detection angle of 9° and 18° was 1.61 s and 1.45 s, respectively. The slope of two-stage partial braking was less than that of one-stage 100% braking. In this case, the initial speed of SV was 90 km/h, and the final impact velocity was 85 km/h, 83 km/h, 80 km/h and 76 km/h, respectively under four different control strategies, as shown in Figure 11b.

The acceleration curves of pre-impact phase under four different control strategies were imported into the validated MADYMO simulation model for occupant kinematics analysis. The X-direction displacements for both occupant's head and T1 were output to evaluate the occupant's kinematics among the pre-impact phase. As shown in Figure 12, the displacements of the head and T1 were increased gradually under the four control strategies. The maximum head and T1 displacements occurred when using the one-stage 100% braking with sensor detection angle of 18°, while the minimum displacements occurred when using the two-stage partial braking with sensor detection angle of 9°. Thus, the braking pressure and sensor detection angle have certain effect on the occupant kinematics during pre-impact phase.

During the pre-impact simulation, the occupant's X-direction displacements were much larger than Z-direction displacements, thus only X-direction displacements were evaluated in this case. Table 1 shows the maximum displacement of each region under four control strategies. It can be concluded that earlier activation of the AEB resulted in larger up-body displacements in this case, and one-stage 100% braking strategy lead to larger up-body displacements than two-stage partial braking strategy. Comparing partial braking with RTA 9° case with 100% braking with RTA 18° case, the head, T1 and shoulder displacements were increased by 94.8%, 104.1% and 48.7%.
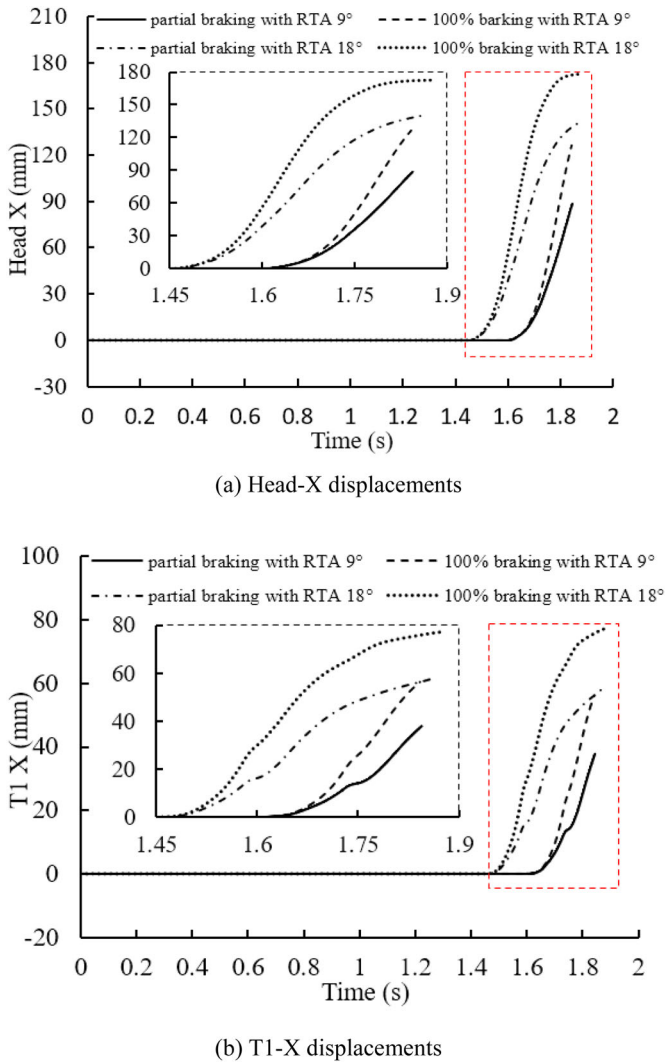
(a) Head-X displacements

(b) T1-X displacements

Figure 12. Occupant head and T1 displacements.

Table 1. The maximum displacement of each region under four control strategies.

Case	Head X(mm)	T1 X(mm)	Shoulder-right X(mm)
Partial braking with RTA 9°	88.57	37.84	29.9
100% braking with RTA 9°	126.42	56.23	33.8
Partial braking with RTA 18°	140.61	57.94	41.6
100% braking with RTA 18°	172.56	77.22	44.45
Average	132.04	57.31	37.42

For further detailed analysis of the occupant's maximum displacements for major regions under four different AEB control strategies, the coordinate point map was drawn by extracting the coordinates from the AHM simulation results, as shown in Figure 13. It can be seen that pre-impact braking affects up-body displacements more obviously than the lower-body displacements. The displacements for pelvis and lower extremity regions were small among the pre-impact braking scenario.

4. Conclusions and discussion

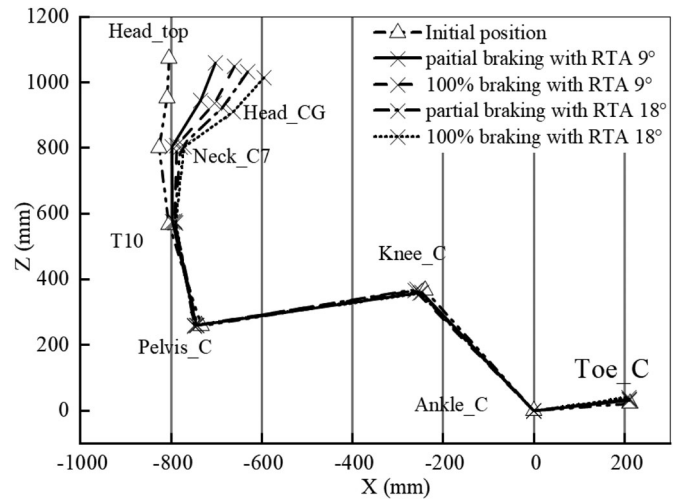This study evaluates the occupant's out-of-position displacements during a typical cut-in scenario and analyzes the

Figure 13. Coordinate point map for certain regions under different AEB control strategies.

effects of AEB control strategy on occupant kinematics. Both the PreScan model for pre-impact vehicle simulation and MADYMO model for occupant kinematics simulation were built. The following conclusions can be drawn:

1. It is efficient to evaluated the occupant kinematics during pre-impact phase through the vehicle and occupant integrated simulation method. For such typical cut-in scenario, the braking manoeuvre by driver (impact speed at 68 km/h) could be more effective than the one controlled by AEB system (the minimum impact speed at 76 km/h).
2. The displacements of active human model and the volunteer are highly consistent among the longitudinal braking, after introducing time dependent muscle activation parameters for occupant simulation model.
3. The pre-impact acceleration affects the occupant's up-body displacements more obvious than pelvis and knee regions in such cut-in scenario. Earlier activation of the AEB results in larger up-body displacements, but less impact velocity for such cut-in scenario. Besides, heavier braking leads to larger up-body displacements.
4. The braking control and sensor detection angle have certain effect on the occupant kinematics during the pre-impact phase. Comparing partial braking with RTA 9° case with 100% braking with RTA 18° case, the head, T1 and shoulder displacements were increased by 94.8%, 104.1% and 48.7%. The maximum head displacement could reach 172.56 mm.

In this case, the main vehicle's velocity was reduced by 5 km/h, 7 km/h, 10 km/h and 14 km/h, respectively when using different AEB control strategies. These control strategies' effectiveness on other driving scenarios need further analysis. Besides, this study only focuses on the occupant longitudinal displacements during the pre-impact phase, the occupant kinematics and injury indexes among the in-crash phase of such typical cut-in scenario requires subsequent study.

Disclosure statement

No potential conflict of interest was reported by the authors.

Funding

References

[1] World Health Organization. Global status report on road safety 2018: summary. Available from: https://www.who.int/violence_injury_prevention/road_safety_status/2018/en/ (accessed December 2018)

[2] Hao L, Heng W, Ting Z, et al. Fine-tuning ADAS algorithm parameters for optimizing traffic safety and mobility in connected vehicle environment. Transp Res Part C Emerg Technol. 2017;76:132–149.

[3] Cao L, Song Z, Ouyang Z, et al. Protection performance analysis and robustness optimization for integrated active and passive seat belt. J Hunan Univ (Nat Sci). 2018;45(10):59–68.

[4] Zhu X, Zhang J, Ma Z. Analysis of driver initial brake time in safety cut-in scenario. China J Highw Transp. 2019;32(6):262–273, 318.

[5] Chen L, Luo Y, Kong W, et al. Occupant injury model for evaluating intelligent driving systems. China J Highw Transp. 2019;32(6):198–205.

[6] Zhang RF, Cao LB, Bao S, et al. A method for connected vehicle trajectory prediction and collision warning algorithm based on V2V communication. Int J Crashworthiness. 2017;22(1):15–25.

[7] McCarthy M, Lange D. A generic evaluation methodoloy for advanced safety systems. Int J Crashworthiness. 2008;13(6):599–607.

[8] Li G, Eben Li S, Cheng B. Field operational test of advanced driver assistance systems in typical Chinese road conditions: the influence of driver gender, age and aggression. Int J Automot Technol. 2015;16(5):739–750.

[9] Kirschbichler S, Huber P, Prüggler A, et al. Factors influencing occupant kinematics during braking and lane change maneuvers in a passenger vehicle. In the IRCOBI conference; 2014. Berlin, Germany.

[10] Gietelink O, Ploeg J, De Schutter B, et al. Development of advanced driver assistance systems with vehicle hardware-in-the-loop simulations. Veh Syst Dyn. 2006;44(7):569–590.

[11] Woitsch G, Sinz W. Influences of pre-crash braking induced dummy – forward displacements on dummy behaviour during EuroNCAP frontal crashtest. Accid Anal Prev. 2014;62:268–275.

[12] Duan J, Li R, Hou L, et al. Driver braking behavior analysis to improve autonomous emergency braking systems in typical Chinese vehicle-bicycle conflicts. Accid Anal Prev. 2017;108:74–82.

[13] Kitagawa Y, Okumura Y, Yamada K. Effectiveness of automatic emergency braking in simulated traffic accident scenarios. In the IRCOBI conference; 2019. Florence, Italy.

[14] Bastien C, Blundell MV, Neal-Sturgess C. A study into the kinematic response for unbelted human occupants during emergency braking. Int J Crashworthiness. 2017;22(6):689–703.

[15] Meijer R, Rodarius C, Adamec J, et al. A first step in computer modelling of the active human response in a far-side impact. Int J Crashworthiness. 2008;13(6):643–652.

[16] Rooij L, Pauwelussen J, Camp O, et al. Driver head displacement during (automatic) vehicle braking tests with varying levels of distraction. In: Proceedings of the 23rd ESV-Conference; 2013. Seoul, Korea.

[17] Bose D, Crandall JR, Untaroiu CD, et al. Influence of pre-collision occupant parameters on injury outcome in a frontal collision. Accid Anal Prev. 2010;42(4):1398–1407.

[18] Huang L, Wang Y, Yang C, et al. Application of Kinovea software in speed calculation of video image. Highw Traffic Technol (Appl Technol). 2015;11(08):210–212.

[19] Hu Y, Zhu H, Zeng X, et al. Analysis of the effect of active retractor parameters on occupant kinematic under braking condition.Automot Eng. 2020;42(05):615-620.

[20] Beeman SM, Kemper AR, Madigan ML, et al. Kinetic and kinematic responses of post mortem human surrogates and the hybrid III ATD in high-speed frontal sled tests. Accid Anal Prev. 2013;55:34–47.

[21] Mages M, Seyffert M. Analysis of the pre-crash benefit of reversible belt prepretensioning in different accident scenarios. In: Proceedings of the 22th ESV-Conference; 2011. Washington, DC.

[22] Yu Y, Jing H, Fan L, et al. Investigation of the effect of neck muscle active force on whiplash injury of the cervical spine. Appl Bionics Biomech. 2018;2018:1–10.

[23] Pithioux M, Chavet P, St-Onge N, et al. Influence of muscle preactivation of the lower limb on impact dynamics in the case of frontal collision. Int J Crashworthiness. 2005;10(6):557–565.

[24] Hill AV. The heat of shortening and the dynamic constants of muscle. Proc R Soc B Biol Sci. 1938;126(843):136–195.

[25] Yamaguchi GT, Sawa AGU, Moran DW, et al. A survey of human musculotendon actuator parameters. In: Winters J.M., Woo S.L.Y. editors. Multiple muscle systems: biomechanics and movement organization. Berlin (Germany): Springer; 1990. p. 717–773.

[26] Winters JM, Stark L. Estimated mechanical properties of synergistic muscles involved in movements of a variety of human joints. J Biomech. 1988;21(12):1027–1041.

[27] Meijer R, Hassel E, Broos J, et al. Development of a multi-body human model that predicts active and passive human behavior. In the IRCOBI conference; 2012. Dublin, Ireland.

[28] Kusano KD, Gabler HC. Safety benefits of forward collision warning, brake assist, and autonomous braking systems in rear-end collisions. IEEE Trans Intell Transp Syst. 2012;13(4):1546–1555.

[29] Bogenrieder R, Fehring M, Bachmann R, et al. Pre-Safe® in rear-end collision situations. In: Proceedings of the 21rd ESV-Conference; 2009. Stuttgart, Germany.

[30] Zhuang J. Automotive electronic control system engineering. Beijing (China): Beijing Institute of Technology Press; 1998. p. 30–148.